Alteration of the cell adhesion molecule L1 expression in a specific subset of primary afferent neurons contributes to neuropathic pain

Hiroki Yamanaka, Koichi Obata, Kimiko Kobayashi, Yi Dai, Tetsuo Fukuoka and Koichi Noguchi

Department of Anatomy and Neuroscience, Hyogo College of Medicine, 1-1 Mukogawa-cho, Nishinomiya, Hyogo 663-8501, Japan

Abstract

The cell adhesion molecule L1 (L1-CAM) plays important functional roles in the developing and adult nervous systems. Here we show that peripheral nerve injury induced dynamic post-transcriptional alteration of L1-CAM in the rat dorsal root ganglia (DRGs) and spinal cord. Sciatic nerve transection (SCNT) changed the expression of L1-CAM protein but not L1-CAM mRNA. In DRGs, SCNT induced accumulation of the L1-CAM into the surface of somata, which resulted in the formation of immunoreactive ring structures in a number of unmyelinated C-fiber neurons. These neurons with L1-CAM-immunoreactive ring structures were heavily colocalized with phosphorylated p38 MAPK. Western blot analysis revealed the increase of full-length L1-CAM and decrease of fragments of L1-CAM after SCNT in DRGs. Following SCNT, L1-CAM-immunoreactive profiles in the dorsal horn showed an increase mainly in pre-synaptic areas of laminae I–II with a delayed onset and colocalized with growth-associated protein 43. In contrast to DRGs, SCNT increased the proteolytic 80-kDa fragment of L1-CAM and decreased full-length L1-CAM in the spinal cord. The intrathecal injection of L1-CAM antibody for the extracellular domain of L1-CAM inhibited activation of p38 MAPK and emergence of ring structures of L1-CAM immunoreactivity in injured DRG neurons. Moreover, inhibition of extracellular L1-CAM binding by intrathecal administration of antibody suppressed the mechanical allodynia and thermal hyperalgesia induced by partial SCNT. Collectively, these data suggest that the modification of L1-CAM in nociceptive pathways might be an important pathomechanism of neuropathic pain.

Introduction

Peripheral nerve injury may lead to neuropathic pain syndromes characterized by both spontaneous and evoked painful sensations. It has been hypothesized that peripheral nerve injury alters the neurochemical features of dorsal root ganglia (DRGs) neurons ('phenotypic change') in both damaged and intact neurons, and results in disordered sensory processing (Zimmermann, 2001; Luo *et al.*, 2002; Obata *et al.*, 2003, 2004a,b; Ji & Strichartz, 2004; Yamanaka *et al.*, 2004). These long-term changes evoked by peripheral nerve injury may lead to the reorganization of dorsal horn circuits and a number of neuroplastic changes. These changes in DRGs and spinal dorsal horn are believed to contribute to the development and maintenance of neuropathic pain (Coderre, 1993; Woolf & Doubell, 1994). The molecular mechanism of how these plastic changes in DRGs and dorsal horn are involved in neuropathic pain states has been a very important theme in pain research.

The neural cell adhesion molecule, cell adhesion molecule L1 (L1-CAM), is a member of the immunoglobulin superfamily and is known to be critical for the development of the nervous system. L1-CAM is involved in a number of processes, including neurite outgrowth (Lemmon *et al.*, 1989; Williams *et al.*, 1992, 1994), axon fasciculation (Kunz *et al.*, 1998; Wiencken-Barger *et al.*, 2004), myelination (Haney *et al.*, 1999) and regeneration in the adult nervous system (Martini & Schachner, 1988; Dihne *et al.*, 2003). L1-CAM binds to a variety of extracellular partners including L1-CAM itself, other members of the immunoglobulin superfamily (Tag1/axonin-1 and contactin/F3/F11) (Kuhn *et al.*, 1991; Brummendorf *et al.*, 1993; Buchstaller *et al.*, 1996), integrins (Ruppert *et al.*, 1995; Montgomery *et al.*, 1996; Thelen *et al.*, 2002) and other extracellular matrix components. Extracellular interactions of L1-CAM with these binding partners have been demonstrated to have physiological significance and lead to the activation of intracellular signaling cascades, such as fibroblast growth factor receptor 1, src, phosphatidylinositol-3′ kinase and MAPK systems (Schaefer *et al.*, 1999; Doherty *et al.*, 2000; Loers *et al.*, 2005). In addition, L1-CAM can participate not only in the development or regeneration of the nervous system but also in the regulation of synaptic plasticity accompanied with circuitry changes in adult rodent brain (Luthl *et al.*, 1994; Saghatelyan *et al.*, 2004). In the nociceptive pathway, L1-CAM is expressed in primary afferent neurons and also in the dorsal horn of spinal cord (Haney *et al.*, 1999; Nakai & Kamiguchi, 2002; Runyan *et al.*, 2005). However, it is not clear how L1-CAM in DRGs and dorsal horn is affected by peripheral nerve injury and whether L1-CAM has a role in the neuropathic pain mechanism. We now show that L1-CAM shows dynamic post-transcriptional modification in DRGs and spinal cord after peripheral nerve injury and is involved in neuropathic pain behaviors by activating intracellular signaling cascades in nociceptive pathways.

Materials and methods

Animal treatment

Male Sprague Dawley rats weighing 200–250 g were anesthetized with sodium pentobarbital (50 mg/kg, i.p.) and received sciatic nerve

transection (SCNT) or partial sciatic nerve transection (PSNL) (Seltzer model). For the SCNT, the left sciatic nerve was transected at the lower thigh level and a 5-mm portion of the nerve was resected to prevent regeneration. For the PSNL, unilateral partial nerve ligation of the sciatic nerve was performed as previously described (Ma & Quirion, 2001). Briefly, a tight ligature was made around the dorsal half of the left sciatic nerve using 8-0 nylon such that half to a third of the sciatic nerve was ligated. The wounds were then closed and the rats were allowed to recover. At several time points (1, 3, 7, 14, 20 and 30 days) following the SCNT, groups of rats were processed for histological analysis ($n = 4$ at each time point). Every effort was made to reduce the number of animals used. All animal experimental procedures were approved by the Hyogo College of Medicine Committee on Animal Research and were carried out in accordance with the National Institutes of Health guidelines on animal care.

Intrathecal administration of anti-cell adhesion molecule L1 antibody

After the SCNT and PSNL, the L6 vertebra was laminectomized and a soft tube (Silascon, Kaneka Medix Company, Osaka, Japan; outer diameter, 0.64 mm) filled with 5 μL of saline was inserted into the subarachnoid space for a length of ∼0.5 cm. After the muscle incision was closed, the mini-osmotic pumps (model 2001 or 2002, Alzet, CA, USA) filled with non-immune mouse IgG (50 μg/mL) diluted by saline, mouse monoclonal antibody against the L1-CAM extracellular domain (R and D Systems Inc., MN, USA) or the p38 inhibitor 4-(4-fluorophenyl)-2-(4-methylsulfonylphenyl)-5-(4-pyridyl)-1H-imidazole (SB203580) (Calbiochem, La Jolla, CA, USA) were connected to the tube. The concentrations of anti-L1-CAM antibody were 0.5, 5 and 50 μg/mL diluted in saline ($n = 6$ for behavioral analysis and $n = 4$ for immunohistochemistry at each drug condition). The pump was then laid under the skin and the incision was closed.

Reverse transcription-polymerase chain reaction

For the reverse transcription-polymerase chain reaction (PCR), the rats were killed by decapitation under deep anesthesia with sodium pentobarbital (50 mg/kg, i.p.) at 0, 3 and 14 days after surgery, and the left L4,5 DRGs were removed and rapidly frozen with powdered dry ice and stored at −80 °C until ready for use ($n = 3$ at each time point). The procedure of extraction of total RNA using the RNA extraction reagent ISOGEN (Nippon Gene, Tokyo, Japan) wasdescribed in our previous study (Fukuoka *et al.*, 2001). PCR primers for L1-CAM and glyceraldehyde 3-phosphate dehydrogenase (GAPDH) cDNA were designed as follows: L1-CAM primers, sense 5′-CCCCAGGTCAC-CATTGGCTA-3′ and antisense 5′-CCCTAAGCCCCGCCCATTAA-3′; GAPDH primers, sense 5′-TGCTGGTGCTGAGTATGTCG-3′ and antisense 5′-GCATGTCAGATCCACAACGG-3′.

The subsequent PCR reaction was performed in a 20-μL solution of 1× PCR buffer (PerkinElmer Life Sciences), 0.2 mM deoxyNTP and 1.25 U of AmpliTaq (PerkinElmer Life Sciences) with a pair of 10-pmol L1-CAM and GAPDH primers on a Perkin DNA Thermal Cycler (PerkinElmer Life Sciences), and the PCR program was 15 s at 94 °C, 15 s at 57 °C and 45 s at 72 °C (Obata *et al.*, 2004b). The intensity of stained bands was measured with a computer-assisted imaging-analysis system (Densitograph, version 4.02; ATTO, Tokyo, Japan). The density of PCR product bands of L1-CAM and GAPDH mRNA was increased between 25 and 35 PCR cycles, depending on the number of cycles; therefore, the number of PCR cycles used was 30. The ratio of L1-CAM : GAPDH mRNA was considered to

indicate the level of each transcript. The mRNA level was expressed as a percentage of the mRNA level in the normal control ganglia. Samples without the addition of reverse transcriptase or without the addition of RNA (negative controls) revealed no detectable product.

In-situ *hybridization*

The protocol for *in-situ* hybridization (ISH) was described in detail previously (Yamanaka *et al.*, 2004). The clone (p-GEM T-easy, Promega, MI, USA) containing a partial sequence corresponding to the coding regions of L1-CAM (from 2495 to 2809, Gene bank Accession no. X59149) was prepared and alpha-^{35}S UTP-labeled antisense and sense cRNA probes were synthesized using the enzyme-digested clones. The ^{35}S-labeled probes in hybridization buffer were placed on the tissue sections on slides. The sections were incubated at 55 °C overnight, then washed and treated with 1 μg/mL RNase A. The sections were then air-dried. After the hybridization reaction, the slides were coated with NTB-3 emulsion (Kodak, Rochester, NY USA) and exposed for 2–5 weeks. Once developed in D-19 (Kodak), the sections were stained with hematoxylin-eosin and coverslipped.

Immunohistochemistry

Rats that received the SCNT or PSNL were used for immunohistochemistry. These rats were deeply anesthetized with sodium pentobarbital (70–80 mg/kg body weight, i.p.) and perfused transcardially with 100 mL of 1% paraformaldehyde in 0.1 M phosphate buffer, pH 7.4, followed by 500 mL of 4% paraformaldehyde in 0.1 M phosphate buffer. The L5 DRGs and spinal cord were dissected out and post-fixed in the same fixative for 4 h at 4 °C, followed by immersion in 30% sucrose in 0.1 M phosphate buffer at 4 °C overnight. The tissue was frozen in powdered dry ice and cut on a cryostat at 25-μm thickness for the spinal cord and 4-μm thickness for the DRGs. The sections were processed for immunohistochemistry using the ABC method (Yamanaka *et al.*, 2004).

The following antibodies were used: goat anti-L1-CAM polyclonal antiserum (1 : 10 000, Santa Cruz Biotechnology, Santa Cruz, CA, USA), rabbit anti-phospho-p38 MAPK (p-p38) polyclonal antiserum (1 : 500, Cell Signaling Technology, Beverly, MA, USA) and rabbit anti-phospho-extracellular signal-regulated kinase polyclonal antiserum (1 : 500, Cell Signaling Technology). Double or triple staining of L1-CAM was performed with the following antibodies; rabbit anti-glial fibrillary acidic protein polyclonal antiserum (1 : 1000, DAKO, Glostrup, Denmark), mouse anti-neurofilament (NF)-200 monoclonal antiserum (1 : 10 000, Sigma, St Louis, MO, USA), mouse anti-synaptophysin monoclonal antiserum (1 : 5000, Chemicon, Temecula, CA, USA), rabbit anti-activating transcription factor 3 (ATF3) polyclonal antiserum (1 : 1000, Santa Cruz Biotechnology), mouse anti-microtubule-associated protein 2 (MAP2) monoclonal antiserum (1 : 5000, Sigma) and mouse anti-growth-associated protein 43 (GAP-43) monoclonal antiserum (1 : 10 000, Sigma).

In brief, DRGs and spinal cord sections were incubated with a mixture of two or three primary antibodies overnight at 4 °C and followed by a mixture of Alexa Fluoro 350, 488 or 594-conjugated secondary antibodies (1 : 5000, Molecular Probes, Eugene, OR, USA) overnight at 4 °C. For double staining of L1-CAM with ATF3, L1-CAM was visualized as black signals by 0.05% 3,3-diaminobenzidine tetrahydrochloride (Sigma) containing 0.3% nickel sulfate and 0.01% hydrogen peroxidase and then ATF3 staining was visualized as

brown signals by the 3,3-diaminobenzidine tetrahydrochloride without nickel sulfate.

Western blot analysis

For the western blot analysis, the rats were killed by decapitation under deep anesthesia with sodium pentobarbital (50 mg/kg, i.p.) at 0, 3 and 14 days after SCNT ($n = 3$ at each time point) and the left DRG and spinal cord were removed and rapidly frozen with powdered dry ice. Frozen spinal cord was homogenized (Polytron PT3000, Brinkmann) at 10% (w/v) in a modified buffer containing 20 mM Tris-HCl, pH 7.4, 10% sucrose and protease inhibitors (protease inhibitor cocktail, 1 : 5000, Nakarai, Kyoto, Japan). Homogenates were vortexed for 60 min with intervening cooling and centrifuged for 60 min at 13 500**g** at 4 °C to recover the supernatant fluid. Proteins were resolved using 10% sodium dodecyl sulfate–polyacrylamide gel electrophoresis and 30 μg protein was applied to each lane. After electrophoresis, proteins were transferred onto a polyvinylidene difluoride membrane (Immobilon-P, Millipore, Bedford, MA, USA) in 125 mM Tris/960 mM glycine for 100 min at 100 mA. Blots were blocked for 1 h in 10% fat-free milk in 0.1 M Tris-buffered saline containing 0.05% Tween 20. Incubations with primary antibodies were performed overnight at 4 °C (polyclonal L1-CAM, 1 : 5000; mouse anti-beta actin monoclonal antiserum, 1 : 10 000, Sigma). Secondary antibodies, IgG conjugated to alkaline phosphatase, were incubated for 1 h at room temperature (25 °C). Signal was detected by chemiluminescence using the Disodium 3-(4-methoxyspiro {1,2-dioxetene-3,2'-(5'-chloro) tricyclo [3.3.1.1^{3,7}] decan}-4-yl) phenyl phosphate ready-to-use reagent (Roche, Indianapolis, IN, USA). Films were scanned and quantified using NIH IMAGE (version 1.61).

Quantification

For quantification of L1-CAM immunoreactivity in the spinal cord, 10 sections of the spinal cord were randomly selected from each rat ($n = 4$ for each group). The immunoreactive (ir) images in laminae I–II were captured with a digital camera and the intensity was measured by a computerized image-analysis system (NIH IMAGE, version 1.61). In 256 gray-scale signal gradients, we considered signal intensities above 192 as positive signals. For quantification of immunostaining in the DRGs (L1-CAM, p-p38 and phospho-extracellular signal-regulated kinase), images were captured by digital camera (for 3,3-diaminobenzidine tetrahydrochloride staining images) and confocal microscopy (for fluorescence images) from each rat ($n = 4$ for each group; a total of at least 500 neurons from each rat), and the immunoreactivities and size of neurons were measured by a computerized image-analysis system (NIH IMAGE, version 1.61). The thresholds of gray level density were set such that only high-intensity ir profiles were accurately discriminated from the low-level ir profiles. Data were represented as mean ± SEM. Differences between groups were compared using one-way ANOVA followed by individual post-hoc comparisons (Fisher's PLSD).

The quantification of ISH was performed as described previously (Yamanaka et al., 2004). Measurements of the density of silver grains over tissue profiles were performed using a computerized image-analysis system (NIH IMAGE, version 1.61). Only neuronal profiles that contained visible nuclei were used for the quantification. At a magnification of 200× and with bright-field illumination, the upper and lower thresholds of gray level density were set such that only silver grains were accurately discriminated from the background in the outlined cell or tissue profile and read by the computer pixel-by-pixel. Next, the area of discriminated pixels was measured and divided by the area of the outlined profile, giving a grain density for each cell or tissue profile. To reduce the risk of biased sampling of the data due to the varying emulsion thickness, we used a signal-to-noise ratio for each cell in each tissue. The signal-to-noise ratio of an individual neuron and its cross-sectioned area that was acquired from the outlined profile was plotted. To distinguish cell size-specific changes, we characterized the DRG neurons as small (< 600 μm^2), medium ($600–1200$ μm^2) and large (> 1200 μm^2), according to their cross-sectional area. As a stereological approach was not used in this study, quantification of the data may represent a biased estimate of the actual numbers of neurons. At least 400 neurons from the L5 DRGs of each rat were measured.

Photomicrographs

All images of ISH and immunohistochemistry with 3,3-diaminobenzidine tetrahydrochloride staining were digitized with a DIAPHOT-300 microscope connected to a DXM-1200 digital camera (both Nikon, Japan). Double- or triple-staining two-dimensional images were acquired using a confocal laser scanning microscope (LSM 510 version 2.8; Carl Zeiss Microimaging, Inc., Germany) with the oil Plan-Neofular 40× and 100× objective lens. We used PHOTOSHOP 6.0 (Adobe Systems, Mountain View, CA, USA) to optimize the images and to make all figures.

Behavioral tests

All PSNL rats were tested for mechanical allodynia and thermal hyperalgesia of the plantar surface of the hindpaw 1 day before surgery and 3, 7, 12, 16 and 21 days after surgery. Mechanical allodynia was assessed with a dynamic plantar aesthesiometer (Ugo Basile, Comerio, Italy), which is an automated von Frey-type system (Kalmar et al., 2003; Lever et al., 2003). To measure mechanical thresholds of the hindpaw, rats were placed in a plastic cage with a wire mesh floor and allowed to acclimate for 15 min before each test session. A paw-flick response was elicited by applying an increasing force (measured in grams) using a plastic filament (0.5 mm diameter) focused on the middle of the plantar surface of the ipsilateral hindpaw. The force applied was initially below the detection threshold, then increased from 1 to 50 g in 1-g steps over 20 s, and was then held at 50 g for an additional 10 s. The rate of force increase was 2.5 g/s. The force to elicit a reflex removal of the ipsilateral hindpaw was monitored. This was defined as the mean of three measurements made at 5-min intervals.

Heat hyperalgesia was tested using the plantar test (7370, Ugo Basile). A radiant heat source beneath a glass floor was aimed at the plantar surface of the hindpaw. Three measurements of latency were taken for each hindpaw in each test session. The hindpaws were tested alternately, with intervals between consecutive tests of 5 min. The three measurements of latency per side were averaged. An assistant, who was unaware of the treatment group, performed all of the behavioral experiments. Data are expressed as mean ± SEM. Differences in changes of values over time of each group were tested using one-way ANOVA, followed by individual post-hoc comparisons (Fisher's PLSD). Pairwise comparisons (Student's t-test) were used to assess the effect of the L1-CAM antibody on the basal mechanical and thermal sensation. A difference was accepted as significant if $P < 0.05$.
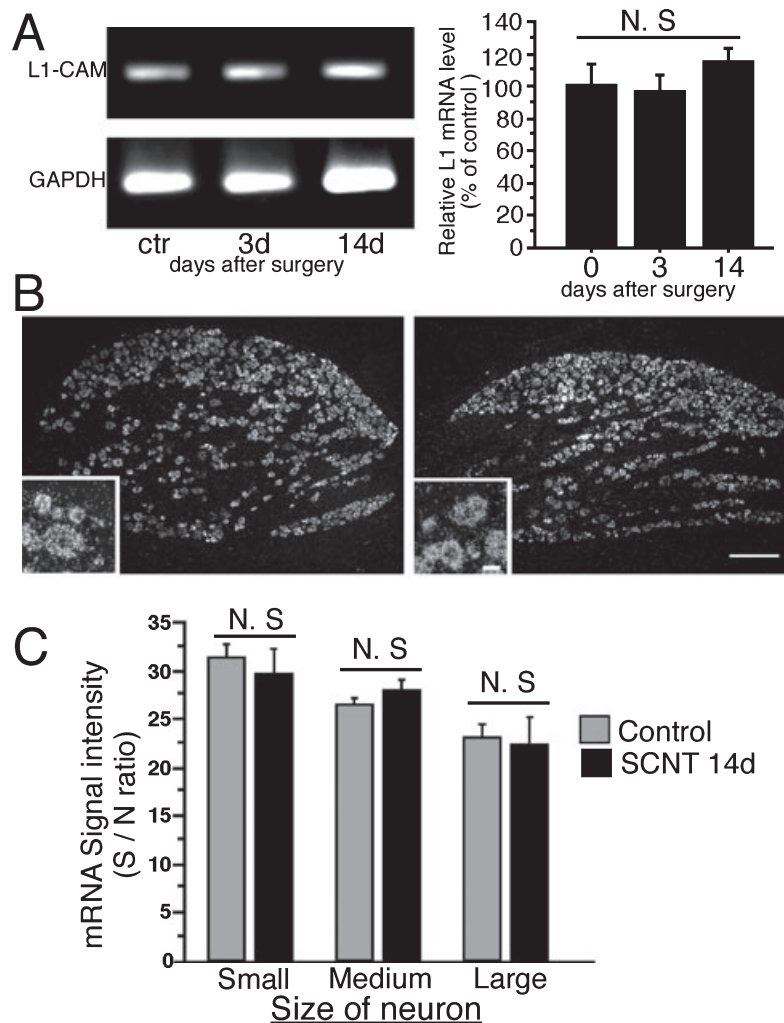
FIG. 1. Expression of cell adhesion molecule L1 (L1-CAM) mRNA in L4,5 dorsal root ganglia (DRGs) after sciatic nerve transection. (A) The levels of L1-CAM mRNA in the ipsilateral L4,5 DRGs were determined by the reverse transcription-polymerase chain reaction (PCR) technique. Gel panels show PCR products from the L4,5 DRGs taken at 3 and 14 days after surgery. Right graph shows the mRNA levels of L1-CAM expressed as percentages of the mRNA level in the normal control ganglia (mean ± SEM). N.S., not significant compared with the naive control ($P > 0.05$; ANOVA). (B) Dark-field images of *in-situ* hybridization (ISH) show L1-CAM mRNA in L5 DRGs of a control rat (left) and 14 days after sciatic nerve transection (SCNT) (right). Insets show highly magnified pictures. (C) Quantification of mean signal density of ISH in each size population in DRG neurons of control rats (grey bars) and 14 days after SCNT (black bars) (mean ± SEM; $n = 4$, total 2099 neurons for SCNT, total 2122 neurons for control naive). N.S., not significant compared with control ($P > 0.05$; Student's *t*-test). Scale bars: 250 μm (low magnification), 25 μm (insets). GAPDH, glyceraldehyde 3-phosphate dehydrogenase.

Results

Peripheral nerve injury did not affect the transcription of cell adhesion molecule L1 mRNA

We used semiquantitative reverse transcription-PCR in order to examine the effect of SCNT on the expression of L1-CAM mRNA in the DRGs. There was no significant change in the quantification of the amplified bands of L1-CAM mRNA after SCNT ($n = 3$ at each time point, Fig. 1A). Expression of L1-CAM mRNA at the cellular level was examined by ISH (Fig. 1B). In the injured and naive DRGs, most neurons expressed L1-CAM mRNA, and weak signals were also observed in satellite cells and Schwann cells. Small- and medium-sized DRG neurons expressed high-intensity signals for L1-CAM mRNA (Fig. 1B and C). The expression of L1-CAM mRNA in DRGs at 14 days after SCNT was similar to the control (Fig. 1B). Quantification of the silver grains on neuronal somata revealed that there were no significant changes in the expression levels of L1-CAM mRNA between the control and SCNT conditions in each size of DRG neurons ($n = 4$, total 2099 and 2122 neurons for SCNT and control rats, respectively, Fig. 1C). We

performed two different exposure conditions for ISH development and obtained similar results (data not shown). These results were consistent with a previous report (Zhang *et al.*, 2000).

Changes of cell adhesion molecule L1 immunostaining in the dorsal root ganglia following sciatic nerve transection

Using anti-L1-CAM antibody, we examined the effect of peripheral axotomy on the expression of L1-CAM protein in the DRGs. In the normal lumbar DRGs, most of the L1-CAM-ir profiles were located in the cytoplasm of a subpopulation of small neurons and axonal fibers (Fig. 2A). Although most of the L1-CAM-ir profiles in small neurons were intensely stained, large neurons showed weak staining. This result was consistent with a previous study (Haney *et al.*, 1999). SCNT led to a marked change in the location of L1-CAM-ir profiles in the ipsilateral DRGs. L1-CAM-ir profiles formed distinct ring structures around cell somata 14 days after SCNT (Fig. 2B). The number of L1-CAM-positive ring structures was significantly
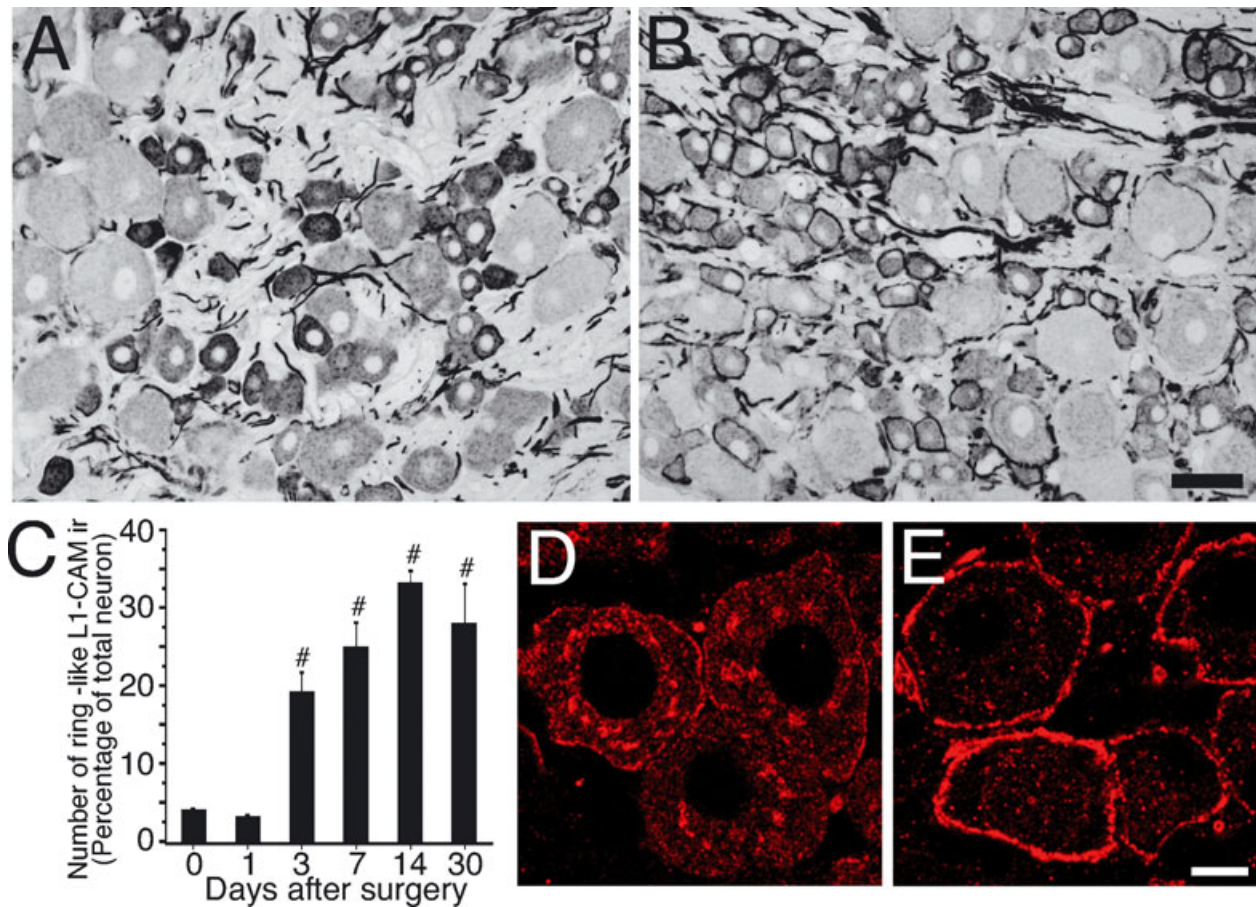
FIG. 2. Changes of cell adhesion molecule L1 (L1-CAM) protein expression and the formation of L1-CAM-immunoreactive (ir) ring structures in the dorsal root ganglia (DRGs) after sciatic nerve transection. Photomicrographs show L1-CAM immunoreactivity in the DRGs of normal control (A) and 14 days after sciatic nerve transection (SCNT) (B). (C) Time course of the formation of L1-CAM-ir ring structures after SCNT shown by the percentage of neurons with L1-CAM-ir ring structures in the total L5 DRGs (mean ± SEM; each time point $n = 4$, more than 500 total neurons from each rat). $\#P < 0.05$ (ANOVA) compared with naive control (day 0). (D and E) Highly magnified confocal two-dimensional images show disappearance of intracellular L1-CAM-ir profiles in DRG neuron and the accumulation around the cytoplasm after SCNT. Control L5 DRG neuron (D) and 14 days after SCNT (E). Scale bars: A and B, 50 μm; D and E, 10 μm.

increased at 3 days after surgery, peaked 7–14 days after injury and then lasted for at least 30 days after SCNT ($n = 4$, more than 2000 neurons at each time point, Fig. 2C). At 14 days after SCNT, $33.3 \pm 1.6\%$ of L5 DRG neurons were surrounded by L1-CAM-positive ring structures. The size distribution analysis revealed that L1-CAM-ir ring structures were located preferentially in small to medium-sized DRG neurons. In the L1-CAM-ir ring structure-positive neurons, $70.1 \pm 4.6\%$ were small ($< 600~\mu m^2$), $19.0 \pm 2.5\%$ were medium (600–$1200~\mu m^2$) and $10.9 \pm 2.7\%$ were large ($> 1200~\mu m^2$) neurons ($n = 4$, total 2079 neurons).

In highly magnified two-dimensional confocal fluorescent images (Fig. 2D), L1-CAM-ir profiles were observed in the cytoplasm that appeared as dots in the control DRGs. These L1-CAM-ir dots were mainly observed in DRG neurons that were intensely labeled for L1-CAM. L1-CAM-ir ring structures were observed in the injured DRGs (Fig. 2E); however, the L1-CAM-ir dots in the cytoplasmic labeling were apparently reduced.

Characterization of cell adhesion molecule L1-immunoreactive ring structures

To identify the cell types that expressed L1-CAM-ir ring structures, we performed double immunostaining of L1-CAM with marker proteins such as glial fibrillary acidic protein (satellite cells) and ATF3 (injured neurons) (Tsujino *et al.*, 2000). NF-200 (myelinated neurons) and p-p38 were examined by triple immunostaining for L1-CAM. We used double labeling with L1-CAM and glial fibrillary acidic protein, a glial marker (Fig. 3A–D), to determine the location of L1-CAM-ir profiles that formed ring structures. The majority of the L1-CAM-ir structures were detected between glial fibrillary acidic protein-positive portions and neuronal somata. In Fig. 1, transcription of L1-CAM was mainly detected in neurons and was at very low levels in satellite cells. Thus, it was considered that the L1-CAM-ir rings were formed on the surface of neuronal somata at day 7 after SCNT (Fig. 3D). Double labeling with L1-CAM and ATF3, a marker of injured neurons, showed that most L1-CAM-ir ring structures were located in ATF3-labeled L5 DRG neurons in the nuclei at 7 days after SCNT (Fig. 3E). Among L1-CAM-ir rings, $87.7 \pm 0.9\%$ of neurons were observed with ATF3-ir nuclei and $68.1 \pm 2.8\%$ of ATF3-ir neurons formed L1-CAM-ir rings ($n = 4$, total of 2305 neurons). Thus, the L1-CAM-positive ring structures were mainly formed on the somata of the injured DRG neurons.

Triple staining with L1-CAM, NF-200 and p-p38 revealed a characteristic expression pattern of the L1-CAM-ir ring structure after SCNT. We found that $26.4 \pm 3.5\%$ of neurons with L1-CAM-ir rings were located around NF-200-ir neurons and L1-CAM-ir rings surrounded $23.4 \pm 4.4\%$ of NF-200-ir neurons (Fig. 3F, H and I). As
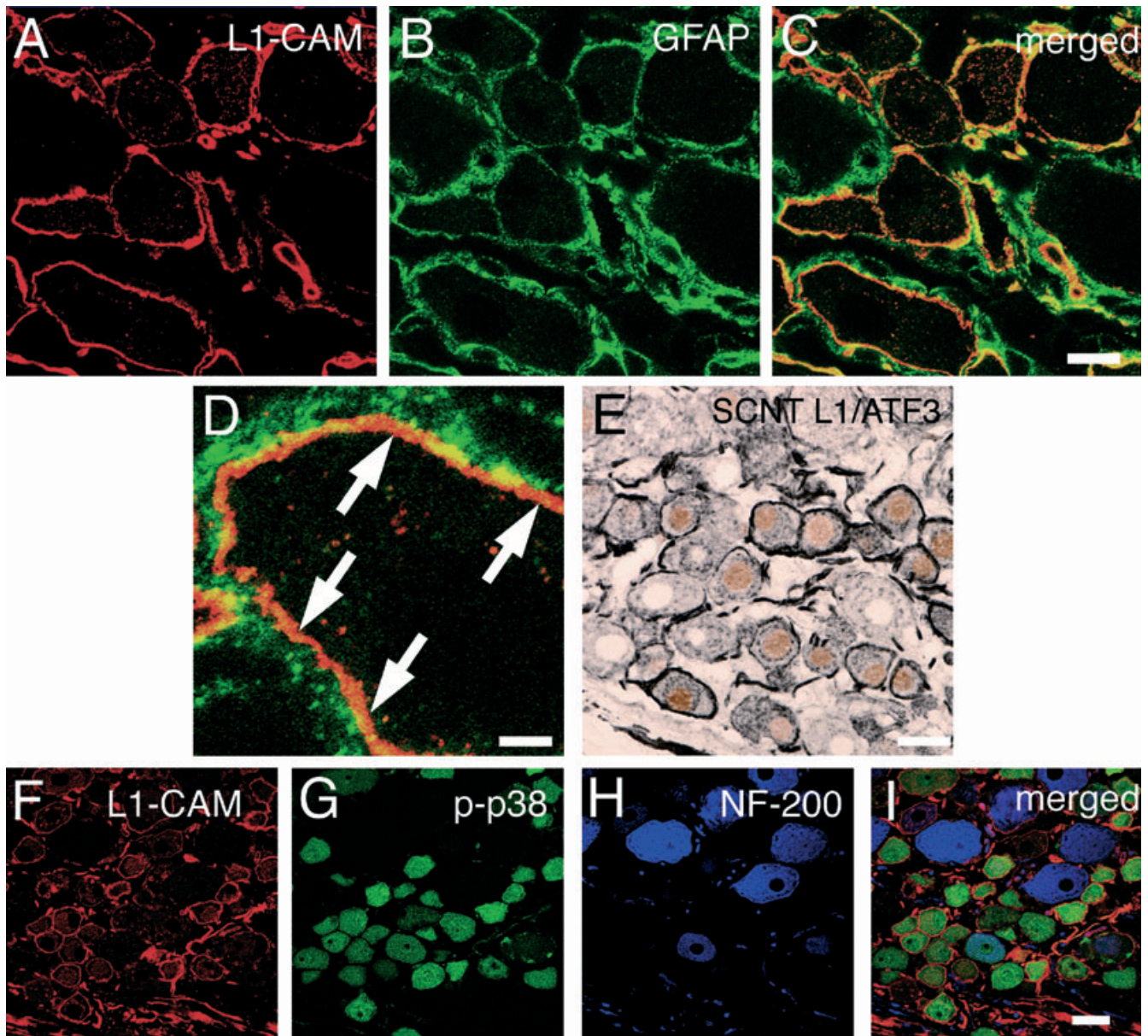
FIG. 3. Characterization of sciatic nerve transection (SCNT)-induced cell adhesion molecule L1 (L1-CAM)-immunoreactive (ir) ring structure in dorsal root ganglia (DRGs). (A–D) Double staining of L1-CAM-ir profiles (red) with glial fibrillary acidic protein (GFAP) (green), a marker of satellite cells and Schwann cells, in the L5 DRGs 7 days after SCNT. (C and D) Merged images of L1-CAM-ir profiles and GFAP-ir staining. (D) Higher magnification image of C. Arrows indicate the L1-CAM-ir profiles that are located in neuronal somata. (E) Double staining of L1-CAM (black) with activating transcription factor 3 (ATF3) (brown), a marker of injured neurons, shows the L1-CAM-ir ring structures formed around injured DRG neurons. (F–I) Triple staining demonstrates heavy colocalization of L1-CAM (red) with phospho-p38 MAPK (p-p38) (green) and not with NF-200 (purple), a marker for myelinated A fibers in injured DRG neurons. Scale bars: A–C, 10 μm; D, 2.5 μm; E, 25 μm; F and G, 25 μm.

NF-200 has been recognized as a marker of DRG neurons with myelinated A-fibers, these data indicated that a majority of the L1-CAM-ir ring structures were formed around C-fiber neurons. p38 MAPK is known to be activated in small DRG neurons after nerve injury and may be involved in neuropathic pain (Jin *et al.*, 2003; Obata *et al.*, 2004a,b). We observed a high incidence of colocalization of L1-CAM and p-p38 at 7 days after SCNT (Fig. 3F, G and I). The quantification showed that $85.3 \pm 0.9\%$ of neurons with the L1-CAM-ir ring structures were labeled for p-p38 and $63.9 \pm 2.4\%$ of p-p38-ir neurons had L1-CAM-ir ring structures ($n = 4$, 586 L1-CAM-ir ring neurons, 770 p-p38-ir neurons and 703 NF-200-ir neurons).

Sciatic nerve transection induced post-transcriptional modification of cell adhesion molecule L1 in dorsal root ganglia

The expression of L1-CAM protein was confirmed by western blot analysis of DRGs using anti-c-terminal L1-CAM. We could detect three bands: 220-kDa (full-length L1-CAM), 105–95-kDa and 80-kDa (c-terminal fragments) proteins. In DRGs, the 105–95-kDa fragments showed a high level of expression. Although the transcription of L1-CAM mRNA did not change after SCNT (Fig. 1), protein levels in DRGs were affected after peripheral nerve injury in DRGs (Fig. 4A, $n = 3$ at each time point). At 3 days after SCNT, the full-length band (220 kDa) increased and continued to 14 days (Fig. 4B). The 105–95-
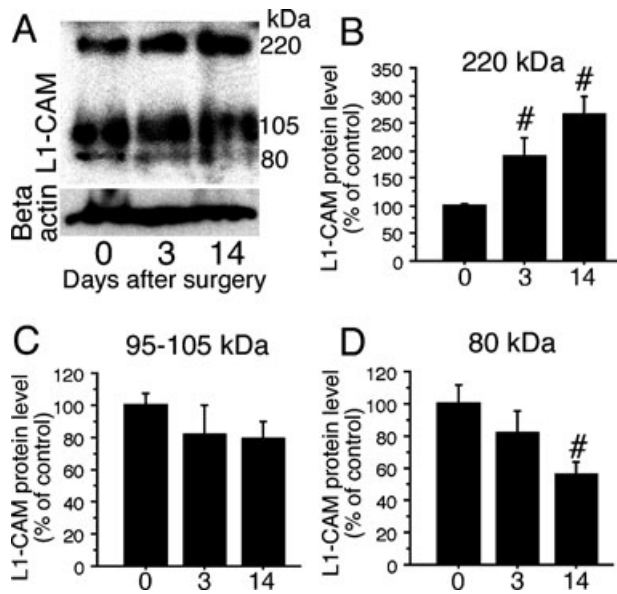
FIG. 4. Alteration of cell adhesion molecule L1 (L1-CAM) fragments in dorsal root ganglia (DRGs) after sciatic nerve transection (SCNT). (A) Western blot analysis indicates an increase in full-length L1-CAM levels and decrease in 80-kDa fragment in DRGs. (B–D) Quantification of the L1-CAM protein levels in DRGs after SCNT. The quantified band length is listed above. $^{#}P < 0.05$ (ANOVA) compared with naive control (day 0).

kDa fragment did not show any changes but the 80-kDa c-terminal fragment showed a significant decrease at 14 days after SCNT (Fig. 4C and D). Clearly, the fragmentation of L1-CAM is altered after peripheral nerve injury.

Cell adhesion molecule L1 increased in the dorsal horn following sciatic nerve transection

The alteration in the localization of L1-CAM immunoreactivity in the dorsal horn was examined after peripheral nerve injury. L1-CAM immunoreactivity in spinal cord was predominantly localized in laminae I–II of the dorsal horn (Fig. 5A and B). In control naive rat, the L1-CAM immunoreactivity was observed as fiber-like or small button-like structures (Fig. 5B). This expression pattern was very similar to the previous study (Munakata *et al.*, 2003; Runyan *et al.*, 2005). SCNT increased the L1-CAM-ir profiles as the large button-like structures and a substantial increase in the number and intensity of L1-CAM-ir buttons were observed in the ipsilateral L4,5 dorsal horn 14 days after SCNT (Fig. 5C and E). The quantification of the L1-CAM-ir buttons revealed that the accumulation of L1-CAM in the dorsal horn became significant at 7 days after SCNT and kept the increase at 20 days ($n = 4$ at each time point). The intensity of the L1-CAM-ir profile on the contralateral side was stable and showed no difference from the control section (Fig. 5E). The increased number of L1-CAM-ir buttons was reduced afterwards and returned to the normal level at 30 days after SCNT (Fig. 5D and E).

Characterization of sciatic nerve transection induced cell adhesion molecule L1-immunoreactive buttons in dorsal horn

To examine the changes in SCNT-induced L1-CAM-ir buttons, we performed double staining of L1-CAM with the markers synaptophysin (pre-synaptic button) and MAP2 (dendrite of second order neuron). SCNT-induced L1-CAM-ir buttons were heavily colocalized with
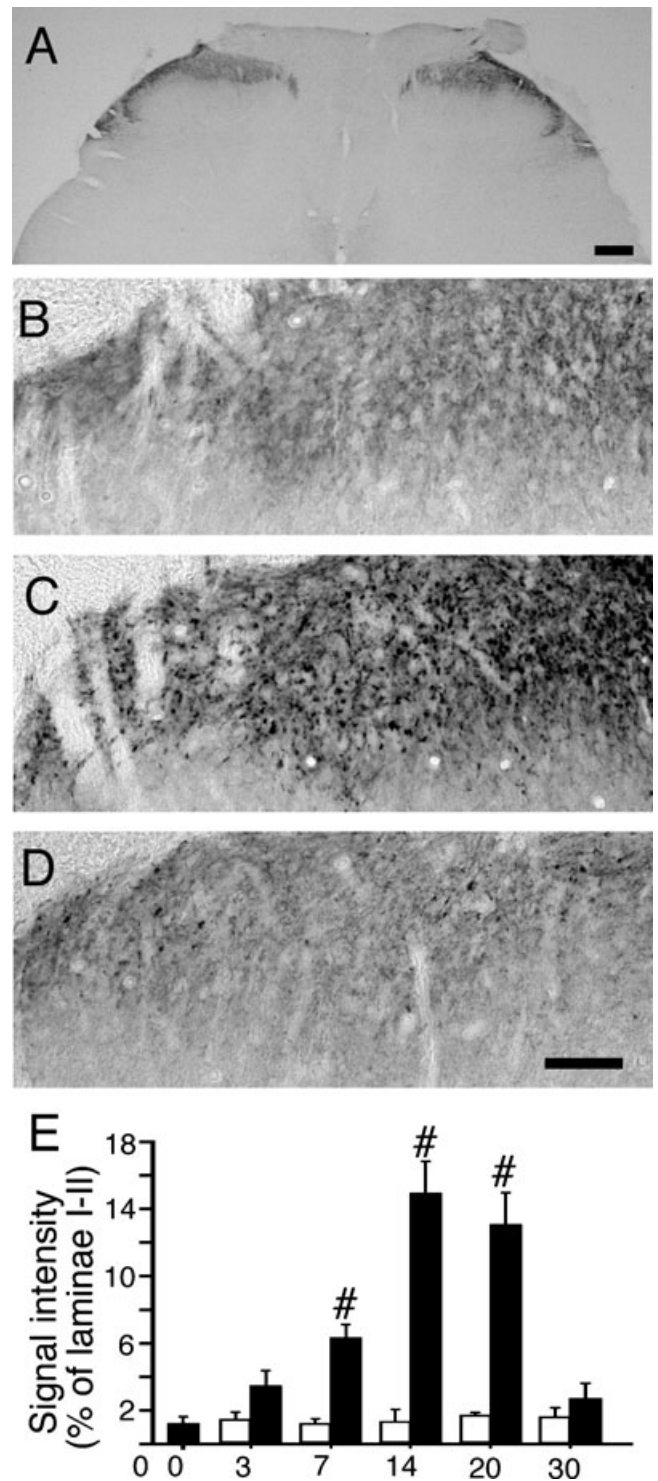

FIG. 5. Increases in cell adhesion molecule L1 (L1-CAM) immunoreactivity in dorsal horn after sciatic nerve transection (SCNT). (A) Low-power magnification images of L1-CAM in spinal cord. Higher magnification images of the dorsal horn in a control naive rat (B), 14 days after SCNT (C) and 30 days after SCNT (D). (C) Increased L1-CAM-immunoreactive (ir) profiles in button-like structures. (E) Statistical quantification shows the effect of SCNT on the area of the L1-CAM-ir buttons per section (mean ± SEM; $n = 4$). $^{#}P < 0.05$ (ANOVA) compared with naive control (day 0). Solid bars: ipsilateral, open bars: contralateral. Scale bars: A, 200 μm; B–D, 50 μm.
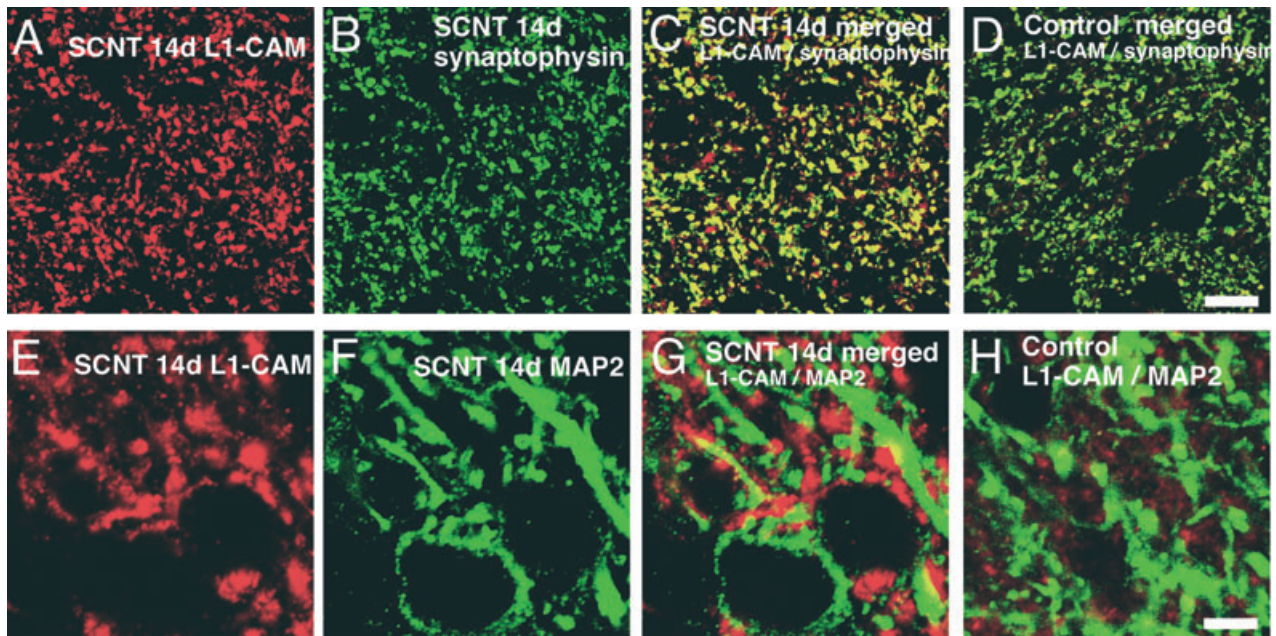
FIG. 6. Characterization of sciatic nerve transection (SCNT)-induced cell adhesion molecule L1 (L1-CAM)-immunoreactive (ir) button in dorsal horn. (A–C) Double staining of L1-CAM (red) with synaptophysin (green), a marker of pre-synaptic buttons, at day 14 after injury shows the increase in L1-CAM-ir profiles in synaptic terminals. (D) Merged image of L1-CAM and synaptophysin in the dorsal horn of control rat. (E–G) Double staining of L1-CAM (red) with microtubule-associated protein 2 (MAP2) (green), a marker of dendrite of central nervous system neuron, at day 14 after SCNT demonstrates L1-CAM accumulation in post-synaptic areas. (H) Merged images of the dorsal horn of control rat. Scale bars: A–D, 10 μm; E–H, 5 μm.

synaptophysin (Fig. 6A–C). In control naive rats, we found a lower basal constitutive expression of L1-CAM and a limited colocalization with synaptophysin (Fig. 6D). Higher magnification confocal images of double labeling with L1-CAM and MAP2 revealed that L1-CAM-ir profiles were attached on MAP2-ir dendrites after SCNT (Fig. 6E–G). In contrast to the SCNT, a very low level of double labeling with L1-CAM and MAP2 was observed in the control naive rats, indicating very little post-synaptic localization of L1-CAM in the control situation (Fig. 6H).

Sciatic nerve transection induced proteolysis of cell adhesion molecule L1 in dorsal horn

The post-transcriptional modification of L1-CAM was examined in the dorsal horn after SCNT. Western blot analysis was performed using extracted protein from the dorsal half portion of the spinal cord ipsilateral to the nerve injury. Three bands of L1-CAM protein were observed in the dorsal horn (Fig. 7A). These fragments were considered to be L1-CAM proteolysed by extracellular proteases (Nayeem *et al.*, 1999; Matsumoto-Miyai *et al.*, 2003). In contrast to the DRGs, the intensity of 105–95 kDa was weak in spinal cord. Densitometric analysis of each band revealed that SCNT affected the proteolysis of L1-CAM in spinal cord ($n = 3$ at each time point); full-length L1-CAM was decreased and the intensity of the 80-kDa band was increased after SCNT (Fig. 7A, B and D). The 105–95-kDa band intensity showed no changes after SCNT (Fig. 7A and C).

Co-localization of sciatic nerve transection induced growth-associated protein 43 and cell adhesion molecule L1 in dorsal horn

As it was reported that peripheral nerve injury induced GAP-43 not only in DRGs but also in laminae I–II of the spinal cord (Woolf *et al.*, 1990; Chong *et al.*, 1994), and GAP-43 plays an essential role in nerve
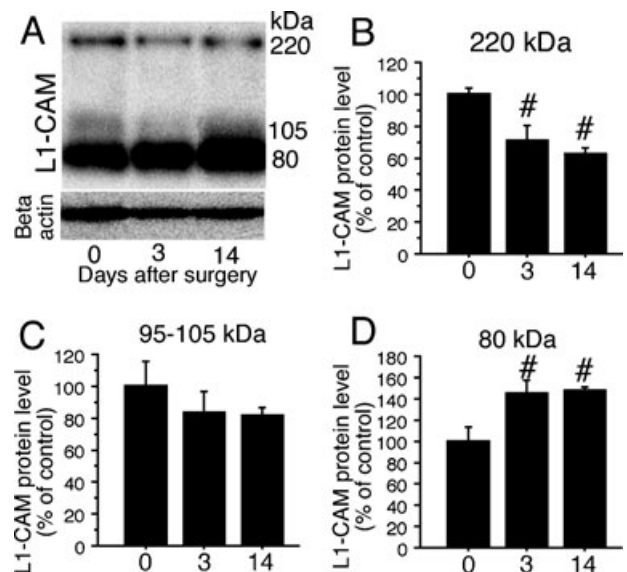

FIG. 7. Proteolysis of cell adhesion molecule L1 (L1-CAM) in the spinal cord after sciatic nerve transection (SCNT). (A) Western blot analysis indicates a decrease in full-length L1-CAM levels and an increase in 80-kDa fragment in dorsal root ganglia (DRGs) after SCNT. (B–D) Quantification of the L1-CAM protein levels in DRGs after SCNT (mean ± SEM; $n = 3$ at each time point). The quantified band lengths are listed above. [#]$P < 0.05$ (ANOVA) compared with naive control (day 0).

regeneration with L1-CAM *in vivo* and *in vitro* (Meiri *et al.*, 1998; Zhang *et al.*, 2005), we examined the colocalization of L1-CAM with GAP-43. After nerve injury, GAP-43 was up-regulated in the ipsilateral laminae I–II of dorsal horn (Fig. 8A and B). Low-power magnification of double-labeling images of GAP-43 with L1-CAM revealed that the up-regulation of GAP-43 was restricted within the
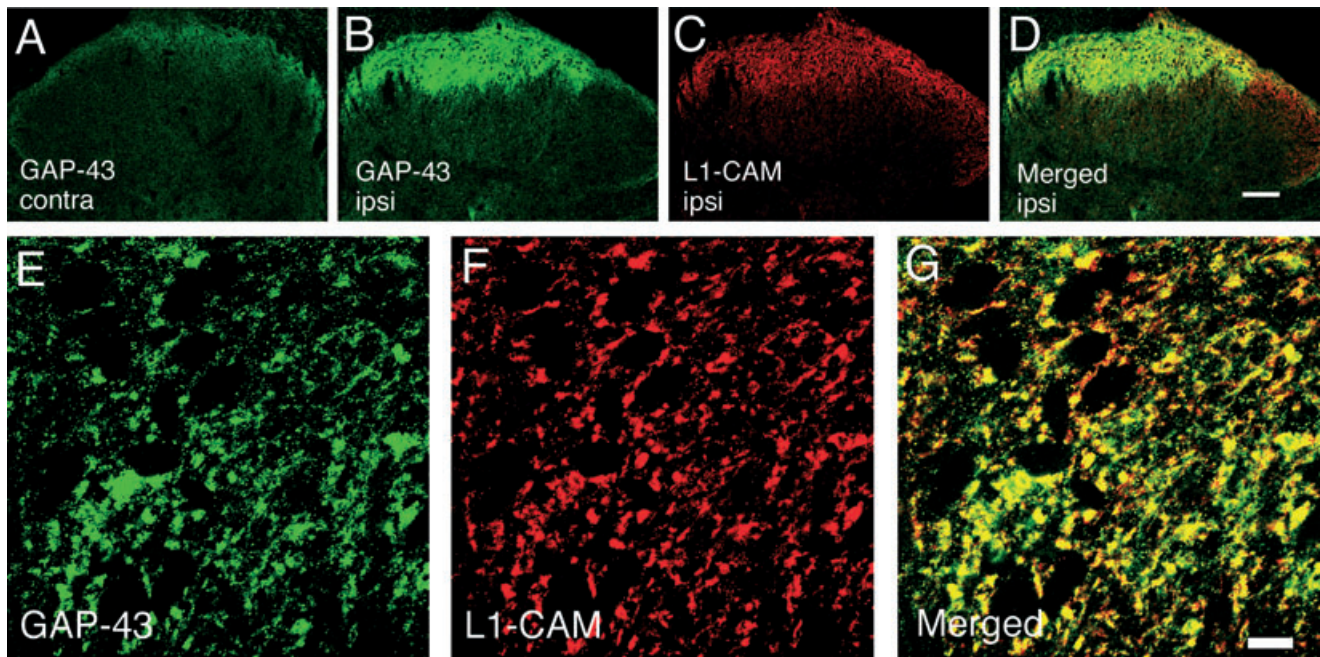
FIG. 8. Double-labeling confocal two-dimensional images of growth-associated protein 43 (GAP-43) (green) and cell adhesion molecule L1 (L1-CAM) (red) in dorsal horn 14 days after sciatic nerve transection (SCNT). (A and B) GAP-43 increased in laminae I–II of the dorsal horn and colocalized with L1-CAM. (A) Contralateral and (B) ipsilateral to the SCNT. (C) L1-CAM immunoreactivity and (D) a merged image of B and C. (E–G) Higher magnification images of double labeling show colocalization with GAP-43- (E) and L1-CAM-immunoreactive buttons (F). (G) A merged image of E and F. Scale bars: A–D, 100 μm; E–G, 10 μm.

L1-CAM-ir positive area (Fig. 8B–D). In the high-power confocal image, most GAP-43 immunoreactivity was observed in the synaptic buttons that expressed L1-CAM (Fig. 8E–G).

Effects of anti-cell adhesion molecule L1 antibody on the formation of cell adhesion molecule L1-immunoreactive ring structures and the activation of p38 MAPK

We have shown that SCNT affected L1-CAM protein expression in DRGs and the dorsal horn synapse and, moreover, the proteolysis of the extracellular domain of L1-CAM (Figs 2, 4, 5 and 7). Next, we examined the effects of intrathecal injection of antibody against the L1-CAM extracellular domain in order to inhibit extracellular interaction of L1-CAM after SCNT. Anti-L1-CAM antibody (600 ng/day) was administrated intrathecally for 5 days in the SCNT model rats ($n = 4$ for each group). We examined the effect of the antibody treatment on the formation of L1-CAM-ir ring structures in DRGs. In control IgG- (600 ng/day) treated rats, the L1-CAM-ir ring structures (visualized by antibody against c-terminal intracellular domain) were significantly increased at 7 days after SCNT when compared with the control naive DRGs (Fig. 9A and B). Anti-L1-CAM extracellular domain antibody treatment significantly suppressed the formation of L1-CAM-ir ring structures in the DRGs (Fig. 9C and D). In the dorsal horn, the increase of L1-CAM-ir buttons was not affected by the anti-L1-CAM antibody treatment (data not shown).

Next, we examined the effect of anti-L1-CAM antibody on the activation of p38 MAPK in the DRGs. Low levels of p-p38-ir neurons were observed ($18.9 \pm 1.6\%$ of DRG neurons) in control naive DRGs (Fig. 9E and H). In the control IgG- (600 ng/day) treated rats, SCNT activated p38 MAPK in a subpopulation of DRG neurons ($41.0 \pm 2.7\%$ of L5 DRG neurons) at 7 days after injury (Fig. 9F and H). Anti-L1-CAM antibody (600 ng/day) administrated

intrathecally by osmotic pump significantly decreased p-p38-ir neurons in the DRGs at 7 days after injury (Fig. 9G and H) ($26.7 \pm 2.8\%$ of L5 DRG neurons, $P < 0.01$). In contrast to the effect on p38 MAPK activation, administration of anti-L1-CAM antibody had no effect on the phosphorylation of extracellular signal-regulated kinase after SCNT. Activation of extracellular signal-regulated kinase in satellite cells and large diameter neurons in the DRGs by peripheral nerve injury was increased compared with naive control (Fig. 9I and J) and intrathecal administration of anti-L1-CAM antibody did not reduce the increase of phospho-extracellular signal-regulated kinase (Fig. 9K and L).

P38 activation did not affect the formation of cell adhesion molecule L1-immunoreactive ring structures in injured dorsal root ganglia

To investigate the contribution of p38 activation to the formation of L1-CAM-ir ring structures, we intrathecally administered the p38 inhibitor SB203580 for 5 days in the SCNT model rats ($n = 4$ for each group). The dose of SB203580 was adjusted as in the previous report (4 μg/day, Jin *et al.*, 2003). SCNT induced ring structures of L1-CAM immunoreactivity in both the control IgG and SB203580-treated DRG sections (Fig. 10A and B). Quantification of the L1-CAM-ir ring structures revealed that the SB203580 treatment had no effect on the formation of L1-CAM-ir ring structures after SCNT ($P > 0.05$, Fig. 10C).

Changes of cell adhesion molecule L1 expression and behavioral hypersensitivity in the neuropathic pain model rats

In PSNL rats that showed pain behaviors, L1-CAM-ir ring structures were exclusively observed in ATF3-ir injured DRG neurons
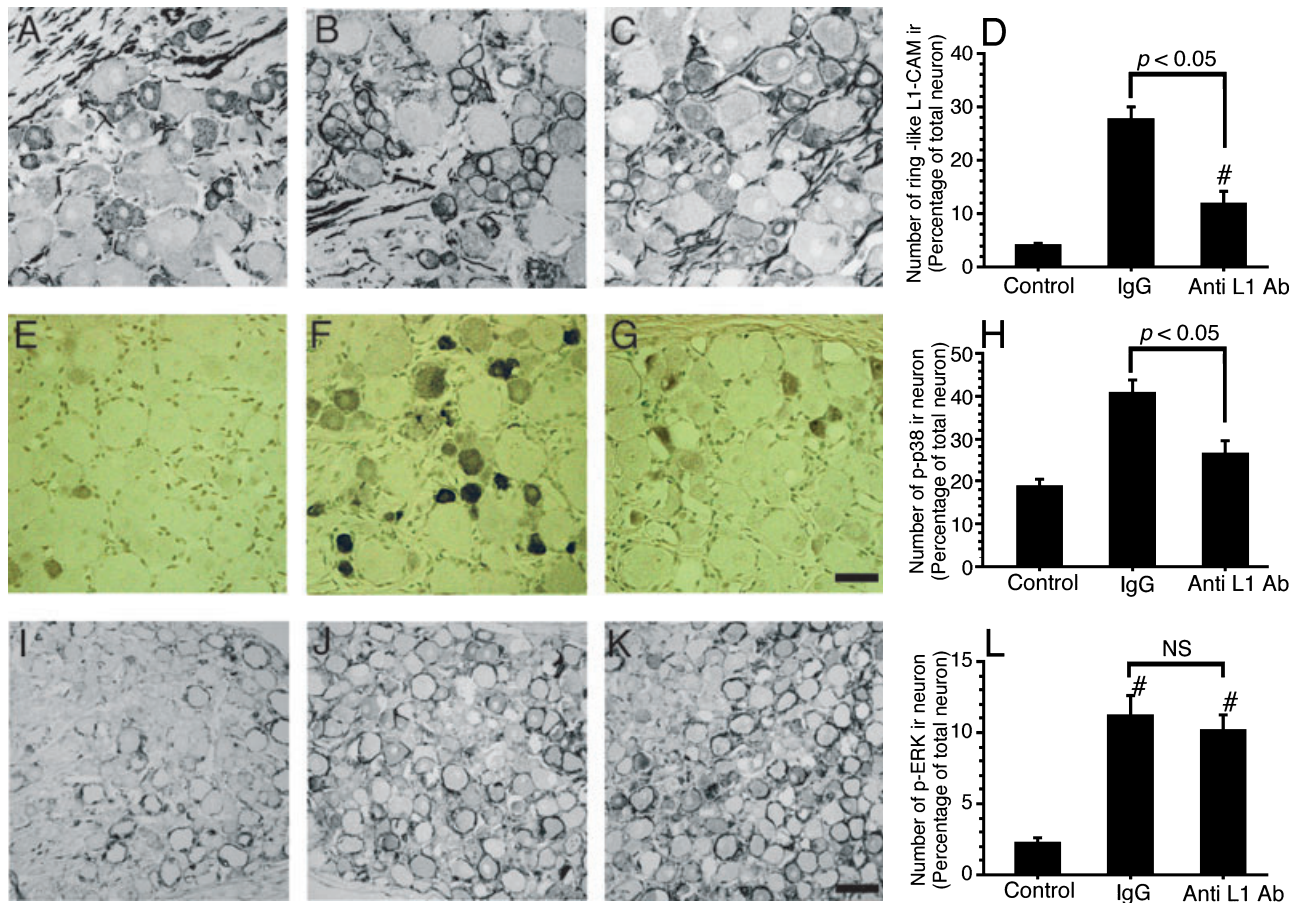
FIG. 9. Effects of the anti-cell adhesion molecule L1 (L1-CAM) antibody on sciatic nerve transection (SCNT)-induced alteration of L1-CAM and phosphorylation of MAPKs in the dorsal root ganglia (DRGs). Photomicrographs show the expression of L1-CAM-immunoreactive (ir) ring structure (A–C), phosphorylated p38-ir profiles (E–G) and phosphorylated extracellular signal-regulated kinase (p-ERK)-ir profiles (I–K). Tissue sections are L5 DRGs of a control naive rat (A, E and I), 7 days after SCNT treatment with intrathecal control IgG (B, F and J) and 7 days after SCNT treatment with intrathecal chronic injection of anti-L1-CAM antibody (600 ng/day) (C, G and K). Quantification of the percentage of neurons with L1-CAM-ir ring structures (D), phospho-p38 MAPK (p-p38)-ir neurons (H) and p-ERK-ir neurons (L) at 7 days after SCNT (mean ± SEM; $n = 4$, more than 500 total neurons from each rat) (Ab, antibody). $P < 0.05$ compared with saline-treated group (ANOVA); NS, not significant ($P > 0.05$); [#]$P < 0.05$ (ANOVA) compared with naive control. Scale bars: A–C and E–G, 50 μm; I–K, 100 μm.

(Fig. 11A). Up-regulation of L1-CAM-ir buttons was also seen in the dorsal horn of the PSNL rats (Fig. 11B). We knew that PSNL, a neuropathic pain model, showed a very similar alteration in L1-CAM expression in DRGs and spinal dorsal horn. In order to investigate whether the alteration of L1-CAM expression is involved in the alteration of nociception and development of neuropathic pain, we examined the effect of intrathecal administration of anti-L1-CAM antibody on the pain behaviors ($n = 6$ for each group). PSNL induced a mechanical allodynia that was present on day 3 after surgery and was maintained for several weeks. We administrated the antibody from day 3 to day 16. The highest dose of anti-L1-CAM antibody administration (600 ng/day) reversed injury-induced mechanical allodynia from day 7 to day 21 after injury (Fig. 11D). In groups with lower concentrations of L1-CAM antibody (60 and 6 ng/day), the significant reduction was observed at 12 and 16 days after injury (Fig. 11D).

Thermal sensitivity was also examined in these animals. PSNL-induced thermal hyperalgesia was attenuated by intrathecal administration of anti-L1-CAM antibody. Thermal hyperalgesia was reversed from day 7 to day 21 after injury when the highest dose was administered (600 ng/day). In lower concentration groups (60 and 6 ng/day), suppression of the thermal hyperalgesia was greater than that of mechanical allodynia. The inhibition of thermal hyperalgesia

produced by the low doses of L1-CAM antibody was observed from day 7 to day 16 (Fig. 11F). In sham-operated rats, the basal mechanical and thermal sensitivity was not affected by the anti-L1-CAM antibody and did not show any difference from the IgG treatment (Fig. 11E and G). The IgG treatment itself did not show any effect.

Anti-cell adhesion molecule L1 antibody reduced cell adhesion molecule L1-immunoreactive ring structures in neuropathic pain model dorsal root ganglia

We confirmed that the anti-L1-CAM antibody treatment inhibited the formation of L1-CAM-ir ring structures in PSNL model DRGs. The expression of L1-CAM was examined following intrathecal administration of anti-L1-CAM antibody or control IgG for 5 days (600 ng/day) in the PSNL model rats ($n = 4$ for each group). Anti-L1-CAM antibody and IgG were administrated from day 2 after injury. The result was similar to the SCNT model. In the control IgG-treated DRGs, a substantial increase of L1-CAM-ir ring structures was observed (Fig. 12A). Intrathecal L1-CAM antibody administration significantly reduced the increase of L1-CAM-ir ring structures (Fig. 12B and C).
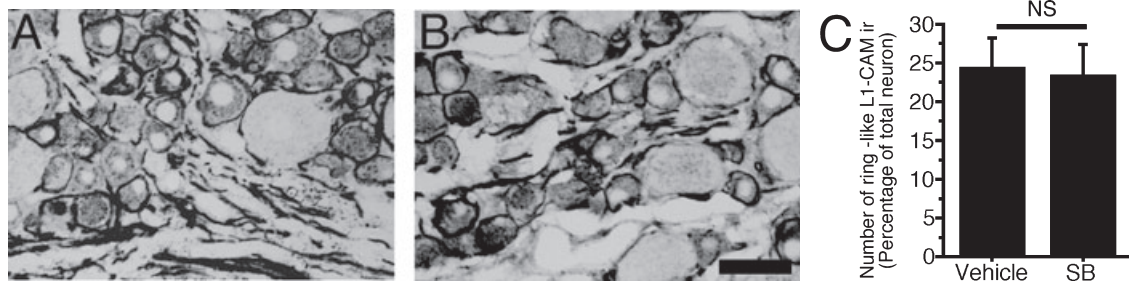
FIG. 10. Effects of the p38 inhibitor 4-(4-fluorophenyl)-2-(4-methylsulfonylphenyl)-5-(4-pyridyl)-1H-imidazole (SB) on the formation of cell adhesion molecule L1 (L1-CAM)-immunoreactive (ir) ring structures in the dorsal root ganglia (DRGs) following sciatic nerve transection (SCNT). Tissue sections are L5 DRGs of 7 days after SCNT treatment with intrathecal control vehicle (A) and 7 days after SCNT treatment with intrathecal chronic injection of SB (4 μg∕day) (B). (C) Quantification of the percentage of neurons with L1-CAM-ir ring structures (mean ± SEM; $n = 4$, more than 500 total neurons from each rat). NS, not significant ($P > 0.05$, Student's t-test). Scale bar, 50 μm.
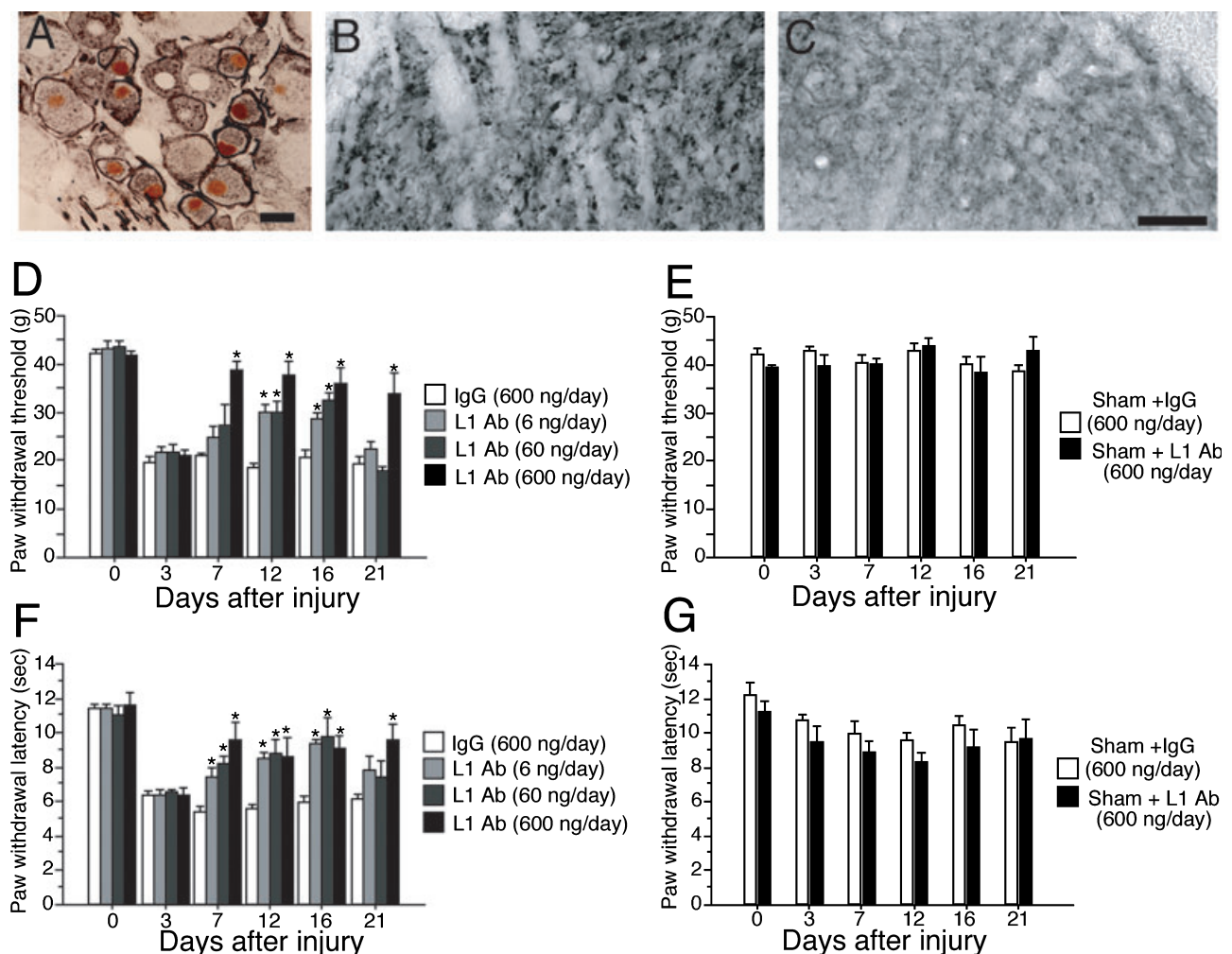

FIG. 11. Changes of cell adhesion molecule L1 (L1-CAM) protein expression and pain behaviors in neuropathic pain model. (A–C) Expression of L1-CAM in dorsal root ganglia (DRGs) and dorsal horn of partial sciatic nerve transection (PSNL) rats at 14 days after injury. (A) Double labeling of L1-CAM with activating transcription factor 3 in DRGs at 14 days after PSNL. (B and C) PSNL induced L1-CAM-immunoreactive buttons in dorsal horn. Dorsal horn ipsilateral (B) and contralateral (C) to the PSNL. Scale bar: A–C, 25 μm. (D–G) Effects of intrathecal chronic administration of anti-L1-CAM antibody on neuropathic pain behaviors. (D) The effects of chronic intrathecal administration of anti-L1-CAM antibody on mechanical allodynia in the PSNL model. The highest concentration of anti-L1-CAM antibody (600 ng∕day) administration reversed the thermal hyperalgesia for up to 21 days after surgery. The lower concentrations of L1-CAM (60 and 6 ng∕day) had a limited effect on the withdrawal threshold, except at day 16 after injury. (F) The withdrawal latency to the radiant heat stimuli was obtained from the same rats that received the mechanical stimuli. Injury-induced thermal hyperalgesia was suppressed by the administration of the L1-CAM antibody. (E and G) Intrathecal anti-L1-CAM antibody and control IgG have no effects on the basal mechanical and thermal sensitivity. *$P < 0.05$ compared with saline-treated group. In all graphs, values were represented by mean ± SEM ($n = 6$ in each group) (Ab, antibody).
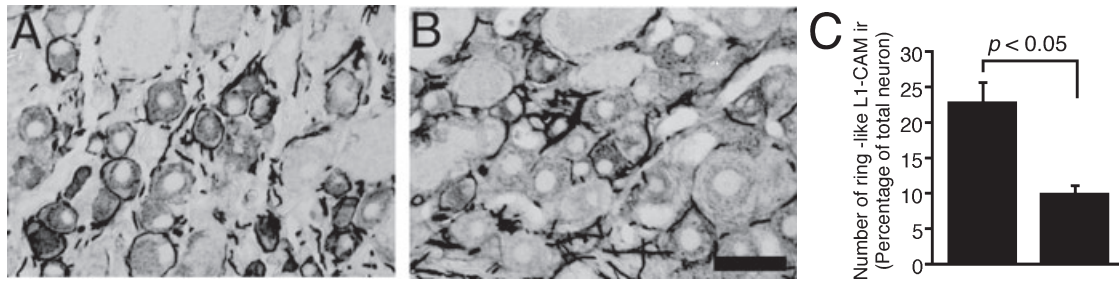
FIG. 12. Effects of the anti-cell adhesion molecule L1 (L1-CAM) antibody on partial sciatic nerve transection (PSNL)-induced alteration of L1-CAM in the dorsal root ganglia (DRGs). Tissue sections are L5 DRGs of 7 days after PSNL treatment with intrathecal control IgG (A) and 7 days after PSNL treatment with intrathecal chronic injection of anti-L1-CAM antibody (600 ng/day) (B). (C) Quantification of the percentage of neurons with L1-CAM-immunoreactive (ir) ring structures (mean ± SEM; $n = 4$, more than 500 total neurons from each rat). $P < 0.05$ compared with control IgG-treated group (Student's *t*-test). Left bar: IgG treatment, right bar: L1-CAM antibody treatment. Scale bar, 50 μm.

Discussion

Changes of cell adhesion molecule L1 expression in injured dorsal root ganglia neurons

Cell adhesion molecule L1 has been shown to exist in the contact surface of injured peripheral axons and wrapping Schwann cells and suggested to be involved in the regeneration process (Martini & Schachner, 1988). The trans-homophilic interaction of L1-CAM may directly promote neurite outgrowth *in vitro* (Lemmon *et al.*, 1989; Doherty *et al.*, 1995). In these studies, L1-CAM was thought to act at the site of regeneration or in neurite elongation. We confirmed that SCNT did not affect the transcription of L1-CAM mRNA and L1-CAM immunoreactivity in cytoplasm was reduced in injured DRG neurons. Therefore, we considered that the appearance of the L1-CAM-ir ring is due to the changes of protein sorting following nerve injury. Accumulated L1-CAM in the cell surface could mediate extracellular signals into the cell body in which the neuronal somata do not receive direct injury. Furthermore, we could show that the peripheral axotomy increased the full-length L1-CAM and decreased the fragments of L1-CAM in DRGs. Therefore, the full-length L1-CAM may accumulate in the surface of somata of DRG neurons after nerve injury. In the present study, it is not clear whether the accumulation of L1-CAM was located only on the neuronal surface or in both neurons and satellite cells after nerve injury. L1-CAM that accumulated in somata might serve as the ligand binding to satellite cells or extracellular matrix.

Previous studies have suggested that neuron–satellite cell communication is mediated by soluble/diffuse factors such as nerve growth factor, nitric oxide or adenosine triphosphate (Aoki *et al.*, 1993; Zhou *et al.*, 1999; Weick *et al.*, 2003; Hanani, 2005). It is known that the damage to peripheral nerves induces satellite cells to promote the neuron–satellite cell interaction and this process between neuron and glial cells has a role in pathological changes in the DRGs after neuropathic injury (Hanani, 2005). Post-transcriptional regulation of L1-CAM, such as the accumulation in neuronal somata and increase of full-length L1-CAM shown in the present study, may be involved in this pathophysiology within DRGs.

Increase of cell adhesion molecule L1 in the dorsal horn after peripheral nerve injury

We showed here that peripheral nerve injury resulted in an increase of L1-CAM mainly in pre-synaptic synapses in the dorsal horn along with the DRGs. When compared with the changes in the DRGs, the increase of synaptic L1-CAM was delayed in time course and occurred after only a short period following nerve injury (7–20 days).

L1-CAM was thought to be involved in synaptic plasticity in the hippocampus (Luthl *et al.*, 1994; Matsumoto-Miyai *et al.*, 2003; Saghatelyan *et al.*, 2004). In mouse brain, a proteomic analysis of *N*-methyl-D-aspartate receptor revealed the molecular link of L1-CAM and *N*-methyl-D-aspartate receptor, and the receptor–adhesion molecule complex was bound to signaling molecules that lead to the MAPK pathway (Husi *et al.*, 2000). *N*-methyl-D-aspartate receptor in the dorsal horn is considered to be one of the key molecules involved in neuropathic pain (Seltzer *et al.*, 1991; Baba *et al.*, 2000). Thus, alterations in L1-CAM in dorsal horn synapses may be involved in the *N*-methyl-D-aspartate receptor activity after peripheral nerve injury.

In dorsal horn synapses, the appearance of pre-synaptic L1-CAM suggests that peripheral nerve injury can affect the dorsal horn neurons by modulating L1-CAM signaling or by dorsal horn circuitry changes mediated by L1-CAM. Western blot analysis showed the increase of the 80-kDa fragment, which may be a product of the cleavage of L1-CAM by plasmin (Nayeem *et al.*, 1999). Our previous study demonstrated that the peripheral nerve injury increased the proteolytic activity of tissue-type plasminogen activator in dorsal horn (Yamanaka *et al.*, 2004). Therefore, peripheral nerve injury can activate the tissue-type plasminogen activator-plasminogen system and this might be a mechanism of cleavage of L1-CAM and increased 80-kDa fragment in the dorsal horn.

Recent studies suggest an interesting hypothesis that the fragment of L1-CAM affects the neuronal activity *in vivo*; the proteolysis of L1-CAM is involved not only in the synaptic plasticity (Matsumoto-Miyai *et al.*, 2003) but also in the neurite outgrowth (Nayeem *et al.*, 1999; Maretzky *et al.*, 2005). In the present study, we confirmed the colocalization of L1-CAM and GAP-43 that is known as a marker for structural plasticity in the central nervous system (Benowitz *et al.*, 1990; Masliah *et al.*, 1991; Li *et al.*, 1998). GAP-43 is known to act synergistically with L1-CAM in neurite outgrowth or regeneration (Meiri *et al.*, 1998; Zhang *et al.*, 2005). Moreover, SCNT rapidly decreased pre-synapse E-cadherin in the dorsal horn (Brock *et al.*, 2004). Collectively, the increase of L1-CAM and reduction of E-cadherin in dorsal horn synapses support the idea that the synaptic reorganization is mediated by the alteration of adhesion molecules after peripheral nerve injury.

Effects of the antibody for cell adhesion molecule L1 on MAPK activation in the dorsal root ganglia and behavioral hypersensitivity

Most L1-CAM-ir ring structures were formed around ATF3-ir neurons, indicating that the emergence of cell surface accumulation

of L1-CAM occurred exclusively in injured neurons. The perturbation of L1-CAM by intrathecal administration of the anti-L1-CAM antibody reduced the L1-CAM-ir ring structure in the DRGs after injury. This suggests that the anti-L1-CAM antibody can inhibit the accumulation of L1-CAM on the cell membrane of neuronal somata and possibly inhibit interaction with satellite cells. In previous reports, anti-L1-CAM antibody was used to inhibit L1-CAM binding, and the blocking of L1-CAM binding suppressed physiologically significant events such as neurite extension, Schwann cell ensheathment, long-term potentiation and remodeling of lymph node reticular matrix during immune response (Seilheimer & Schachner, 1988; Seilheimer *et al.*, 1989; Luthl *et al.*, 1994; Di Sciullo *et al.*, 1998). Thus, we believe that the effects of the anti-L1-CAM antibody shown in the present study are the result of L1-CAM binding inhibition in the nociceptive pathways. The mechanism of how the antibody treatment reduced the accumulation of L1-CAM on the cell surface needs further study. It may be due to the internalization of accumulated L1-CAM by the antibody binding as demonstrated *in vitro* (Schmid *et al.*, 2000).

We also demonstrated that the intrathecal injection of the anti-L1-CAM antibody reduced activation of p38 MAPK but not phospho-extracellular signal-regulated kinase in the injured DRGs. We previously reported that SCNT activated extracellular signal-regulated kinase in large diameter neurons and satellite cell in DRGs (Obata *et al.*, 2003). These cells do not seem to colocalize with L1-CAM-ir ring structures in DRGs. *In-vitro* studies demonstrate that L1-CAM can activate extracellular signal-regulated kinase (Doherty *et al.*, 2000). The discrepancy of these results is not clear at this point. The reduction of activated p38 MAPK by the anti-L1-CAM antibody treatment is intriguing because p-p38 was induced in DRG neurons after nerve injury and is thought to be one of the factors responsible for neuropathic pain (Jin *et al.*, 2003; Obata *et al.*, 2004a,b). The finding that inhibition of L1-CAM results in a reduction of both the cell surface accumulation of L1-CAM and the activation of p38 MAPK suggested a possible interaction between L1-CAM accumulation and activation of p38 MAPK. There are two major L1-CAM signaling pathways, the fibroblast growth factor receptor 1–phospho-lipase C gamma-mediated pathway (Doherty *et al.*, 1995; Meiri *et al.*, 1998) and the *src*-dependent MAPK pathway (Schmid *et al.*, 2000). There have been no reports showing that these fibroblast growth factor receptor 1 and *src*-signaling cascades can activate p38 MAPK in the DRGs. The present data indicate that the extracellular interaction by L1-CAM in injured neurons may activate intracellular signaling cascades such as p38 MAPK and affect the neuroplastic changes in the DRGs and spinal dorsal horn, resulting in the pain hypersensitivity in neuropathic conditions.

In order to determine the effect of the alteration of L1-CAM on pain behaviors, we intrathecally injected an antibody for the L1-CAM extracellular domain. Although the anti-L1-CAM antibody did not affect basal pain sensitivity, both mechanical and thermal hyperalgesia were significantly suppressed in a dose-dependent manner from 4 days after initiation of antibody administration until 1 week after the termination of the administration. At the doses that we used, we did not find obvious toxicity of this antibody, animals behaved normally and locomotion was unaffected. These data suggest that the suppression of L1-CAM binding by antibody administration can affect the pain hypersensitivity in a partial nerve injury model and the alteration in L1-CAM in primary afferents is involved in the development of neuropathic pain. The intrathecal antibody could not suppress the increase of L1-CAM-ir buttons in the dorsal horn. The facts that the infused antibody is for the extracellular domain and the increased button consists of mainly proteolytic fragments of L1-CAM could be one reason for the ineffectiveness. However, we cannot exclude a possible role of L1-CAM changes in the dorsal horn on pain behaviors in the neuropathic pain model. The accumulation of the L1-CAM in neural somata and synapses may mediate cell–cell interaction and the communication of neurons and satellite cells. The possible involvement of L1-CAM in the activation of p38 MAPK and synaptic reorganization represents a novel form of modulation of nociceptive pathways.

Abbreviations

ATF3, activating transcription factor 3; DRG, dorsal root ganglion; GAP-43, growth-associated protein 43; GAPDH, glyceraldehyde 3-phosphate dehydrogenase; ir, immunoreactive; ISH, *in-situ* hybridization; L1-CAM, cell adhesion molecule L1; MAP2, microtubule-associated protein 2; NF-200, neurofilament-200; PCR, polymerase chain reaction; p-p38, phospho-p38 MAPK; PSNL, partial sciatic nerve ligation; SB203580, 4-(4-fluorophenyl)-2-(4-methylsulfonylphenyl)-5-(4-pyridyl)-1H-imidazole; SCNT, sciatic nerve transection.

References

Aoki, E., Takeuchi, I.K., Shoji, R. & Semba, R. (1993) Localization of nitric oxide-related substances in the peripheral nervous tissues. *Brain Res.*, **620**, 142–145.

Baba, H., Doubell, T.P., Moore, K.A. & Woolf, C.J. (2000) Silent NMDA receptor-mediated synapses are developmentally regulated in the dorsal horn of the rat spinal cord. *J. Neurophysiol.*, **83**, 955–962.

Benowitz, L.I., Perrone-Bizzozero, N.I., Neve, R.L. & Rodriguez, W. (1990) GAP-43 as a marker for structural plasticity in the mature CNS. *Prog. Brain Res.*, **86**, 309–320.

Brock, J.H., Elste, A. & Huntley, G.W. (2004) Distribution and injury-induced plasticity of cadherins in relationship to identified synaptic circuitry in adult rat spinal cord. *J. Neurosci.*, **24**, 8806–8817.

Brummendorf, T., Hubert, M., Treubert, U., Leuschner, R., Tarnok, A. & Rathjen, F.G. (1993) The axonal recognition molecule F11 is a multi-functional protein: specific domains mediate interactions with Ng-CAM and restrictin. *Neuron*, **10**, 711–727.

Buchstaller, A., Kunz, S., Berger, P., Kunz, B., Ziegler, U., Rader, C. & Sonderegger, P. (1996) Cell adhesion molecules NgCAM and axonin-1 form heterodimers in the neuronal membrane and cooperate in neurite outgrowth promotion. *J. Cell Biol.*, **135**, 1593–1607.

Chong, M.S., Reynolds, M.L., Irwin, N., Coggeshall, R.E., Emson, P.C., Benowitz, L.I. & Woolf, C.J. (1994) GAP-43 expression in primary sensory neurons following central axotomy. *J. Neurosci.*, **14**, 4375–4384.

Coderre, T.J. (1993) The role of excitatory amino acid receptors and intracellular messengers in persistent nociception after tissue injury in rats. *Mol. Neurobiol.*, **7**, 229–246.

Dihne, M., Bernreuther, C., Sibbe, M., Paulus, W. & Schachner, M. (2003) A new role for the cell adhesion molecule L1 in neural precursor cell proliferation, differentiation, and transmitter-specific subtype generation. *J. Neurosci.*, **23**, 6638–6650.

Di Sciullo, G., Donahue, T., Schachner, M. & Bogen, S.A. (1998) L1 antibodies block lymph node fibroblastic reticular matrix remodeling in vivo. *J. Exp. Med.*, **187**, 1953–1963.

Doherty, P., Williams, E. & Walsh, F.S. (1995) A soluble chimeric form of the L1 glycoprotein stimulates neurite outgrowth. *Neuron*, **14**, 57–66.

Doherty, P., Williams, G. & Williams, E.J. (2000) CAMs and axonal growth: a critical evaluation of the role of calcium and the MAPK cascade. *Mol. Cell Neurosci.*, **16**, 283–295.

Fukuoka, T., Kondo, E., Dai, Y., Hashimoto, N. & Noguchi, K. (2001) Brain-derived neurotrophic factor increases in the uninjured dorsal root ganglion neurons in selective spinal nerve ligation model. *J. Neurosci.*, **21**, 4891–4900.

Hanani, M. (2005) Satellite glial cells in sensory ganglia: from form to function. *Brain Res. Brain Res. Rev.*, **48**, 457–476.

Haney, C.A., Sahenk, Z., Li, C., Lemmon, V.P., Roder, J. & Trapp, B.D. (1999) Heterophilic binding of L1 on unmyelinated sensory axons mediates Schwann cell adhesion and is required for axonal survival. *J. Cell Biol.*, **146**, 1173–1184.

Husi, H., Ward, M.A., Choudhary, J.S., Blackstock, W.P. & Grant, S.G. (2000) Proteomic analysis of NMDA receptor-adhesion protein signaling complexes. *Nat. Neurosci.*, **3**, 661–669.

Ji, R.R. & Strichartz, G. (2004) Cell signaling and the genesis of neuropathic pain. *Sci. STKE*, **250**, re 14.

Jin, S.X., Zhuang, Z.Y., Woolf, C.J. & Ji, R.R. (2003) p38 mitogen-activated protein kinase is activated after a spinal nerve ligation in spinal cord microglia and dorsal root ganglion neurons and contributes to the generation of neuropathic pain. *J. Neurosci.*, **23**, 4017–4022.

Kalmar, B., Greensmith, L., Malcangio, M., McMahon, S.B., Csermely, P. & Burnstock, G. (2003) The effect of treatment with BRX-220, a co-inducer of heat shock proteins, on sensory fibers of the rat following peripheral nerve injury. *Exp. Neurol.*, **184**, 636–647.

Kuhn, T.B., Stoeckli, E.T., Condrau, M.A., Rathjen, F.G. & Sonderegger, P. (1991) Neurite outgrowth on immobilized axonin-1 is mediated by a heterophilic interaction with L1(G4). *J. Cell Biol.*, **115**, 1113–1126.

Kunz, S., Spirig, M., Ginsburg, C., Buchstaller, A., Berger, P., Lanz, R., Rader, C., Vogt, L., Kunz, B. & Sonderegger, P. (1998) Neurite fasciculation mediated by complexes of axonin-1 and Ng cell adhesion molecule. *J. Cell Biol.*, **143**, 1673–1690.

Lemmon, V., Farr, K.L. & Lagenaur, C. (1989) L1-mediated axon outgrowth occurs via a homophilic binding mechanism. *Neuron*, **2**, 1597–1603.

Lever, I., Cunningham, J., Grist, J., Yip, P.K. & Malcangio, M. (2003) Release of BDNF and GABA in the dorsal horn of neuropathic rats. *Eur. J. Neurosci.*, **18**, 1169–1174.

Li, Y., Jiang, N., Powers, C. & Chopp, M. (1998) Neuronal damage and plasticity identified by microtubule-associated protein 2, growth-associated protein 43, and cyclin D1 immunoreactivity after focal cerebral ischemia in rats. *Stroke*, **29**, 1972–1980.

Loers, G., Chen, S., Grumet, M. & Schachner, M. (2005) Signal transduction pathways implicated in neural recognition molecule L1 triggered neuroprotection and neuritogenesis. *J. Neurochem.*, **92**, 1463–1476.

Luo, Z.D., Calcutt, N.A., Higuera, E.S., Valder, C.R., Song, Y.H., Svensson, C.I. & Myers, R.R. (2002) Injury type-specific calcium channel alpha 2 delta-1 subunit up-regulation in rat neuropathic pain models correlates with antiallodynic effects of gabapentin. *J. Pharmacol. Exp. Ther.*, **303**, 1199–1205.

Luthl, A., Laurent, J.P., Figurov, A., Muller, D. & Schachner, M. (1994) Hippocampal long-term potentiation and neural cell adhesion molecules L1 and NCAM. *Nature*, **372**, 777–779.

Ma, W. & Quirion, R. (2001) Increased phosphorylation of cyclic AMP response element-binding protein (CREB) in the superficial dorsal horn neurons following partial sciatic nerve ligation. *Pain*, **93**, 295–301.

Maretzky, T., Schulte, M., Ludwig, A., Rose-John, S., Blobel, C., Hartmann, D., Altevogt, P., Saftig, P. & Reiss, K. (2005) L1 is sequentially processed by two differently activated metalloproteases and presenilin / gamma-secretase and regulates neural cell adhesion, cell migration, and neurite outgrowth. *Mol. Cell Biol.*, **25**, 9040–9053.

Martini, R. & Schachner, M. (1988) Immunoelectron microscopic localization of neural cell adhesion molecules (L1, N-CAM, and myelin-associated glycoprotein) in regenerating adult mouse sciatic nerve. *J. Cell Biol.*, **106**, 1735–1746.

Masliah, E., Fagan, A.M., Terry, R.D., DeTeresa, R., Mallory, M. & Gage, F.H. (1991) Reactive synaptogenesis assessed by synaptophysin immunoreactivity is associated with GAP-43 in the dentate gyrus of the adult rat. *Exp. Neurol.*, **113**, 131–142.

Matsumoto-Miyai, K., Ninomiya, A., Yamasaki, H., Tamura, H., Nakamura, Y. & Shiosaka, S. (2003) NMDA-dependent proteolysis of presynaptic adhesion molecule L1 in the hippocampus by neuropsin. *J. Neurosci.*, **23**, 7727–7736.

Meiri, K.F., Saffell, J.L., Walsh, F.S. & Doherty, P. (1998) Neurite outgrowth stimulated by neural cell adhesion molecules requires growth-associated protein-43 (GAP-43) function and is associated with GAP-43 phosphorylation in growth cones. *J. Neurosci.*, **18**, 10 429–10 437.

Montgomery, A.M., Becker, J.C., Siu, C.H., Lemmon, V.P., Cheresh, D.A., Pancook, J.D., Zhao, X. & Reisfeld, R.A. (1996) Human neural cell adhesion molecule L1 and rat homologue NILE are ligands for integrin alpha v beta 3. *J. Cell Biol.*, **132**, 475–485.

Munakata, H., Nakamura, Y., Matsumoto-Miyai, K., Itoh, K., Yamasaki, H. & Shiosaka, S. (2003) Distribution and densitometry mapping of L1-CAM immunoreactivity in the adult mouse brain − light microscopic observation. *BMC Neurosci.*, **4**, art. 7.

Nakai, Y. & Kamiguchi, H. (2002) Migration of nerve growth cones requires detergent-resistant membranes in a spatially defined and substrate-dependent manner. *J. Cell Biol.*, **159**, 1097–1108.

Nayeem, N., Silletti, S., Yang, X., Lemmon, V.P., Reisfeld, R.A., Stallcup, W.B. & Montgomery, A.M. (1999) A potential role for the plasmin(ogen) system in the posttranslational cleavage of the neural cell adhesion molecule L1. *J. Cell Sci.*, **112**, 4739–4749.

Obata, K., Yamanaka, H., Dai, Y., Tachibana, T., Fukuoka, T., Tokunaga, A., Yoshikawa, H. & Noguchi, K. (2003) Differential activation of extracellular signal-regulated protein kinase in primary afferent neurons regulates brain-derived neurotrophic factor expression after peripheral inflammation and nerve injury. *J. Neurosci.*, **23**, 4117–4126.

Obata, K., Yamanaka, H., Dai, Y., Mizushima, T., Fukuoka, T., Tokunaga, A. & Noguchi, K. (2004a) Differential activation of MAPK in injured and uninjured DRG neurons following chronic constriction injury of the sciatic nerve in rats. *Eur. J. Neurosci.*, **20**, 2881–2895.

Obata, K., Yamanaka, H., Kobayashi, K., Dai, Y., Mizushima, T., Katsura, H., Fukuoka, T., Tokunaga, A. & Noguchi, K. (2004b) Role of mitogen-activated protein kinase activation in injured and intact primary afferent neurons for mechanical and heat hypersensitivity after spinal nerve ligation. *J. Neurosci.*, **24**, 10 211–10 222.

Runyan, S.A., Roy, R., Zhong, H. & Phelps, P.E. (2005) L1 CAM expression in the superficial dorsal horn is derived from the dorsal root ganglion. *J. Comp. Neurol.*, **485**, 267–279.

Ruppert, M., Aigner, S., Hubbe, M., Yagita, H. & Altevogt, P. (1995) The L1 adhesion molecule is a cellular ligand for VLA-5. *J. Cell Biol.*, **131**, 1881–1891.

Saghatelyan, A.K., Nikonenko, A.G., Sun, M., Rolf, B., Putthoff, P., Kutsche, M., Bartsch, U., Dityatev, A. & Schachner, M. (2004) Reduced GABAergic transmission and number of hippocampal perisomatic inhibitory synapses in juvenile mice deficient in the neural cell adhesion molecule L1. *Mol. Cell Neurosci.*, **26**, 191–203.

Schaefer, A.W., Kamiguchi, H., Wong, E.V., Beach, C.M., Landreth, G. & Lemmon, V. (1999) Activation of the MAPK signal cascade by the neural cell adhesion molecule L1 requires L1 internalization. *J. Biol. Chem.*, **274**, 37 965–37 973.

Schmid, R.S., Pruitt, W.M. & Maness, P.F. (2000) A MAP kinase-signaling pathway mediates neurite outgrowth on L1 and requires Src-dependent endocytosis. *J. Neurosci.*, **20**, 4177–4188.

Seilheimer, B. & Schachner, M. (1988) Studies of adhesion molecules mediating interactions between cells of peripheral nervous system indicate a major role for L1 in mediating sensory neuron growth on Schwann cells in culture. *J. Cell Biol.*, **107**, 341–351.

Seilheimer, B., Persohn, E. & Schachner, M. (1989) Antibodies to the L1 adhesion molecule inhibit Schwann cell ensheathment of neurons in vitro. *J. Cell Biol.*, **109**, 3095–3103.

Seltzer, Z., Cohn, S., Ginzburg, R. & Beilin, B. (1991) Modulation of neuropathic pain behavior in rats by spinal disinhibition and NMDA receptor blockade of injury discharge. *Pain*, **45**, 69–75.

Thelen, K., Kedar, V., Panicker, A.K., Schmid, R.S., Midkiff, B.R. & Maness, P.F. (2002) The neural cell adhesion molecule L1 potentiates integrin-dependent cell migration to extracellular matrix proteins. *J. Neurosci.*, **22**, 4918–4931.

Tsujino, H., Kondo, E., Fukuoka, T., Dai, Y., Tokunaga, A., Miki, K., Yonenobu, K., Ochi, T. & Noguchi, K. (2000) Activating transcription factor 3 (ATF3) induction by axotomy in sensory and motoneurons: a novel neuronal marker of nerve injury. *Mol. Cell Neurosci.*, **15**, 170–182.

Weick, M., Cherkas, P.S., Hartig, W., Pannicke, T., Uckermann, O., Bringmann, A., Tal, M., Reichenbach, A. & Hanani, M. (2003) P2 receptors in satellite glial cells in trigeminal ganglia of mice. *Neuroscience*, **120**, 969–977.

Wiencken-Barger, A.E., Mavity-Hudson, J., Bartsch, U., Schachner, M. & Casagrande, V.A. (2004) The role of L1 in axon pathfinding and fasciculation. *Cereb. Cortex*, **14**, 121–131.

Williams, E.J., Doherty, P., Turner, G., Reid, R.A., Hemperly, J.J. & Walsh, F.S. (1992) Calcium influx into neurons can solely account for cell contact-dependent neurite outgrowth stimulated by transfected L1. *J. Cell Biol.*, **119**, 883–892.

Williams, E.J., Furness, J., Walsh, F.S. & Doherty, P. (1994) Activation of the FGF receptor underlies neurite outgrowth stimulated by L1, N-CAM, and N-cadherin. *Neuron*, **13**, 583–594.

Woolf, C.J. & Doubell, T.P. (1994) The pathophysiology of chronic pain − increased sensitivity to low threshold A beta-fibre inputs. *Curr. Opin. Neurobiol.*, **4**, 525–534.

Woolf, C.J., Reynolds, M.L., Molander, C., O'Brien, C., Lindsay, R.M. & Benowitz, L.I. (1990) The growth-associated protein GAP-43 appears in dorsal root ganglion cells and in the dorsal horn of the rat spinal cord following peripheral nerve injury. *Neuroscience*, **34**, 465–478.

Yamanaka, H., Obata, K., Fukuoka, T., Dai, Y., Kobayashi, K., Tokunaga, A. & Noguchi, K. (2004) Tissue plasminogen activator in primary afferents induces dorsal horn excitability and pain response after peripheral nerve injury. *Eur. J. Neurosci.*, **19**, 93–102.

Zhang, Y., Roslan, R., Lang, D., Schachner, M., Lieberman, A.R. & Anderson, P.N. (2000) Expression of CHL1 and L1 by neurons and glia following sciatic nerve and dorsal root injury. *Mol. Cell Neurosci.*, **16**, 71–86.

Zhang, Y., Bo, X., Schoepfer, R., Holtmaat, A.J., Verhaagen, J., Emson, P.C., Lieberman, A.R. & Anderson, P.N. (2005) Growth-associated protein GAP-43 and L1 act synergistically to promote regenerative growth of Purkinje cell axons in vivo. *Proc. Natl Acad. Sci. U.S.A.*, **102**, 14 883–14 888.

Zhou, X.F., Deng, Y.S., Chie, E., Xue, Q., Zhong, J.H., McLachlan, E.M., Rush, R.A. & Xian, C.J. (1999) Satellite-cell-derived nerve growth factor and neurotrophin-3 are involved in noradrenergic sprouting in the dorsal root ganglia following peripheral nerve injury in the rat. *Eur. J. Neurosci.*, **11**, 1711–1722.

Zimmermann, M. (2001) Pathobiology of neuropathic pain. *Eur. J. Pharmacol.*, **429**, 23–37.